

NJC

Accepted Manuscript



This is an *Accepted Manuscript*, which has been through the Royal Society of Chemistry peer review process and has been accepted for publication.

Accepted Manuscripts are published online shortly after acceptance, before technical editing, formatting and proof reading. Using this free service, authors can make their results available to the community, in citable form, before we publish the edited article. We will replace this *Accepted Manuscript* with the edited and formatted *Advance Article* as soon as it is available.

You can find more information about *Accepted Manuscripts* in the [Information for Authors](#).

Please note that technical editing may introduce minor changes to the text and/or graphics, which may alter content. The journal's standard [Terms & Conditions](#) and the [Ethical guidelines](#) still apply. In no event shall the Royal Society of Chemistry be held responsible for any errors or omissions in this *Accepted Manuscript* or any consequences arising from the use of any information it contains.

Cite this: DOI: 10.1039/c0xx00000x

www.rsc.org/xxxxxx

ARTICLE TYPE

Tailoring π -Conjugated Dithienosilole–Benzothiadiazole Oligomers for Organic Solar Cells

Xuelong Huang, Guichuan Zhang, Cheng Zhou, Shengjian Liu, Jie Zhang, Lei Ying,* Fei Huang,* Yong Cao

Received (in XXX, XXX) Xth XXXXXXXXX 20XX, Accepted Xth XXXXXXXXX 20XX

DOI: 10.1039/b000000x

A series of donor-acceptor type of π -conjugated oligomers based on dithieno[3,2-*b*;2',3'-*d*]silole as the electron donor and 2,1,3-benzothiadiazole as the electron acceptor were designed and synthesized. It was found that the elongation of the molecular lengths of chromophores can significantly influence the thermal properties, UV-vis absorption, electrochemical properties, and photovoltaic performances of fabricated organic solar cells. The higher molecular weight chromophore exhibited narrower band gap than those lower molecular weight counterparts. Solution processed bulk-heterojunction organic solar cells were fabricated with inverted device structure of ITO/PFN-OX/oligomer:PCBM/MoO₃/Al, where the best device performance was achieved with power conversion efficiency of 1.12%. These results indicated that the elongation of the molecular length of π -conjugated small-molecules can be an effective strategy for the improvement of organic photovoltaic performance of narrow band-gap chromophores.

1 Introduction

Over the past decade, organic photovoltaics (OPVs) have attracted much attention due to their great potential for the fabrication of low-cost, light weight and flexible devices.¹⁻³ Recently, remarkable progress by virtue of relatively high power conversion efficiency over 10% has been reached on the basis of bulk-heterojunction (BHJ) architectures in the photoactive layer.⁴⁻⁷ In general, the BHJ architectures comprised fullerene derivatives such as [6,6]-phenyl-C61-butyric acid methyl ester (PC₆₁BM) or [6,6]-phenyl-C71-butyric acid methyl ester (PC₇₁BM) as electron-accepting materials, and various narrow band-gap π -conjugated small-molecules or polymers as the electron-donating materials. With respect to the polymeric counterparts, π -conjugated small-molecules are of particular interests not singly due to their easily tailoring molecular structures that can lead to competitive device performances, but also owing to their specific advantages of precise synthesis and purification that can avoid batch-to-batch variations.⁸⁻¹¹ Despite the well-extended absorbance, appropriate energy levels, high charge-carrier mobility and desirable phase separation can be attained based on these conjugated small molecules,¹²⁻¹⁴ the device performances in terms of power conversion efficiencies are still lag behind those based on conjugated polymers¹⁵⁻¹⁷. These issues lead to the necessity of systematically elucidating structure–property relationships of such chromophores, which is critically important and can provide the guideline for future molecular design.¹⁸⁻²³

It is well-established that the dithieno[3,2-*b*;2',3'-*d*]silole (DTS) and 2,1,3-benzothiadiazole (BT) moieties can act as promising building blocks for the construction of high-performance π -conjugated small-molecules and polymers.^{11,22} For

instance, Liu et al. developed a series of narrow band gap conjugated chromophores comprising DTS, BT and various electron-deficient moieties in the molecular backbone, and systematically investigate the influence of the molecular architectures on the thermal resistance, self-organization, and charge carrier mobility and optoelectronic properties.²⁴ Liu et al. also developed several DTS/BT based conjugated chromophores by incorporating fluorine substitutions to study the effect of molecular fluorination on bulk thermal properties relevant to optoelectronic device applications.²⁵ While a wide range of conjugated small molecules comprising DTS and BT units have been developed, less efforts have been devoted to investigate the influence of extended π -conjugation on the electronic properties and device performances of molecules basically consisted with DTS and BT unit.

In this article, we report the synthesis, characterization, and photovoltaic application of a series of donor-acceptor (D-A) type of π -conjugated oligomers on the basis of DTS as the electron-donating unit (D) and BT as the electron-accepting unit (A), which was briefly denoted as DA, ADA, DAD, DADAD. The molecular framework of the DTS-based oligomers varied with the conjugation length and end groups. It was also realized that the elongation of the molecular length can have great impact on the UV-vis absorption, molecular orbital energy levels, film morphologies, as well as the performances of the fabricated organic solar cells.

2. Experimental

2.1. Measurement and characterization

The ¹H and ¹³C NMR spectra were collected on a Bruker AV-300 (300 MHz) in deuterated chloroform solution with

tetramethylsilane as an internal standard. Matrix-assisted laser desorption/ionization time-of-flight (MALDI-TOF) mass spectra were recorded with a Bruker Daltonics BIFLEX III MODLI-TOF analyzer. UV-vis spectra were obtained with a Shimadzu UV-3600 spectrophotometer. Thermogravimetric analysis (TGA) was carried out with a Netzsch TG 209 under N₂ flow at a heating rate of 10 °C min⁻¹. Surface roughness and morphology of thin films were characterized by atomic force microscopy (AFM) on an Agilent 5400. For cyclic voltammetry (scan rate 50 mV cm⁻¹), the electrochemical apparatus consisted of a CHI660B electrochemical workstation, platinum working electrodes, counter electrode and a saturated calomel reference electrode (SCE).

2.2. Device fabrication and characterization

The organic photovoltaic cells was constructed in the form of the inverted structure of glass/indium tin oxide (ITO)/PFN-OX/oligomer:PCBM/MoO₃/Al.²⁶ The ITO-coated glass substrates were cleaned in an ultrasonic bath with deionized water, acetone, and isopropyl alcohol and dried in a nitrogen stream, followed by an oxygen plasma treatment. To fabricate photovoltaic devices, a thin layer (~40 nm) of poly[9,9-bis(6,6'-(*N,N*-diethylamino)hexyl)fluorene-*alt*-9,9-bis(3-ethyl(oxetane-3-ethyloxy)hexyl)fluorene] (PFN-OX) was spin-coated on the pre-cleaned glass substrates at 5000 rpm and baked at 140 °C for 10 min under ambient conditions.²⁷ The substrates were then transferred into an argon-filled glove box. A blend solution of the oligomers and PC₆₁BM or PC₇₁BM with different weight ratios were prepared in the mixture of 1,2-dichlorobenzene and chloroform. Subsequently, the solutions were spin-coated onto the PFN-OX coated ITO substrate to form the active layer about 100 nm. To complete device fabrication, a 3 nm MoO₃ layer and an 80 nm Al were thermally evaporated onto the active layer through shadow masks. The effective area was measured to be 0.15 cm².

2.3. Synthesis of intermediates and target oligomers

All chemicals and reagents were purchased from either Aldrich or Alfa-Aesar, and the reactions and manipulations were carried out under a dry argon atmosphere. All the materials were used as received unless specified. Tetrahydrofuran (THF) was distilled from sodium before use. Toluene was dried by anhydrous magnesium sulfate before use. 4,4'-Bis-(*n*-octyl)dithieno[3,2-*b*:2',3'-*d*]silole²⁸, 4-bromo-2,1,3-benzothiadiazole (**1**)²⁹, 4,7-dibromo-2,1,3-benzothiadiazole (**2**)²⁹, 4,4'-bis(*n*-octyl)-5-trimethyltin-dithieno[3,2-*b*:2',3'-*d*]silole (**3**)²⁸, 4,4'-bis(*n*-octyl)-5,5'-bis(trimethyltin)-dithieno[3,2-*b*:2',3'-*d*]silole (**4**)²⁸ were prepared according to the published procedures. All oligomers were purified by silica column and high performance liquid chromatography (HPLC) for device characterization.

Oligomer DA. A solution of compound 1 (0.288 g, 1.34 mmol) and compound 3 (0.779 g, 1.34 mmol) in toluene (20 mL) was degassed twice with argon followed by the addition of Pd(PPh₃)₄ (3 mol%). After being stirred at 80 °C for 18 h under argon, the reaction mixture was poured into deionized water (100 mL) and extracted with dichloromethane. The organic layer was washed with water and then dried over anhydrous MgSO₄. After removal of solvent, the crude product was purified by column chromatography on silica gel using a mixture of dichloromethane and petroleum ether (1/30 in v/v) as eluent to give the target compound DA (0.26 g, 35 %). ¹H NMR (300 MHz, CDCl₃) δ=8.11 (s, 1H), 7.89-7.83 (m, 2H), 7.61 (dd, *J* = 7.25 and 8.78 Hz, 1H),

7.27 (d, *J* = 4.8 Hz, 1H), 7.10 (d, *J* = 4.8 Hz, 1H), 1.50-0.80 (m, 34H); ¹³C NMR (75 MHz, CDCl₃) δ=155.60, 152.06, 142.85, 142.42, 139.77, 130.56, 129.76, 128.04, 125.99, 124.52, 119.33, 118.16, 33.18, 31.86, 29.21, 29.17, 24.11, 22.65, 14.08, 11.19. MS (MALDI-TOF): calcd. for C₃₀H₄₀N₂S₃Si [M]⁺: 552.21; found, 552.075.

Oligomer ADA. Compound 4 (0.877 g, 1.18 mmol), compound 1 (0.634 g, 2.95 mmol) and Pd(PPh₃)₄ (3 mol%) were dissolved in 30 mL of dry toluene. The mixture was stirred overnight at 80 °C, the solvent was evaporated and the product was purified by column chromatography on silica with petroleum ether/dichloromethane (5/1 in v/v) as the eluent. The solvent was evaporated and compound ADA was obtained as a dark red solid (0.3 g, 37 %). ¹H NMR (300 MHz, CDCl₃) δ= 8.16 (s, 2H), 7.86 (m, 4H), 7.57 (dd, *J* = 7.18 and 8.67 Hz, 2H), 1.50-0.80 (m, 34H); ¹³C NMR (75 MHz, CDCl₃) δ= 155.58, 152.02, 150.62, 143.66, 140.85, 130.70, 129.65, 127.90, 124.59, 119.43, 33.19, 31.85, 29.22, 29.19, 24.25, 22.63, 14.02, 11.99. MS (MALDI-TOF): calcd. for C₃₆H₄₂N₄S₄Si [M]⁺: 686.21; found, 686.147.

Oligomer DAD. Compound 3 (2.15 g, 3.69 mmol), compound 2 (0.435 g, 1.48 mmol) and Pd(PPh₃)₄ (4 mol%) were dissolved in 30 mL of dry THF. The mixture was stirred overnight at 80 °C, the solvent was evaporated and the product was purified by column chromatography on silica with petroleum ether/dichloromethane (20/1 in v/v) as the eluent. The solvent was evaporated and compound DAD was obtained. (0.5 g, 35 %). ¹H NMR (300 MHz, CDCl₃) δ= 8.11 (s, 2H), 7.85 (s, 2H), 7.28 (d, *J* = 4.8 Hz, 2H), 7.11 (d, *J* = 4.8 Hz, 2H), 1.50-0.80 (m, 68H); ¹³C NMR (75 MHz, CDCl₃) δ= 152.76, 150.92, 149.46, 143.20, 142.65, 140.40, 130.29, 130.02, 126.19, 125.91, 125.23, 33.43, 32.09, 29.45, 29.41, 24.45, 22.88, 14.32, 12.16. MS (MALDI-TOF): calcd. for C₅₄H₇₆N₂S₅Si₂ [M]⁺: 968.42; found, 968.290.

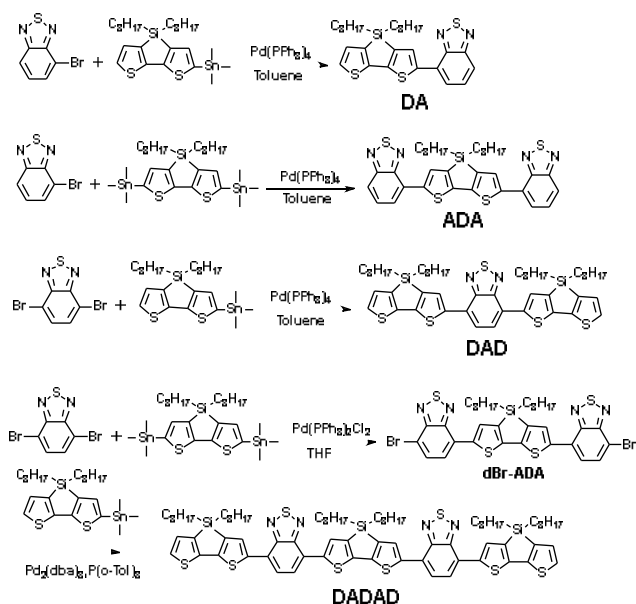
Compound dBr-ADA. Compound 4 (0.88 g, 1.18 mmol), compound 2 (1.74 g, 5.92 mmol) and Pd(PPh₃)₂Cl₂ (2.76 mol%) were dissolved in 30 mL of dry THF. The mixture was stirred overnight at 80 °C, the solvent was evaporated and the product was purified by column chromatography on silica with petroleum ether/dichloromethane (5/1 in v/v) as the eluent. The solvent was evaporated and compound dBr-ADA was obtained as a dark red solid (0.34 g, 31 %). ¹H NMR (300 MHz, CDCl₃) δ= 8.13 (s, 2H), 7.83 (d, *J* = 8.0 Hz, 2H), 7.69 (d, *J* = 8.0 Hz, 2H), 1.50-0.80 (m, 34H); ¹³C NMR (75 MHz, CDCl₃) δ= 153.58, 150.91, 144.05, 140.24, 132.37, 130.91, 127.36, 125.00, 111.65, 33.19, 31.85, 29.70, 29.23, 24.21, 22.65, 14.07, 11.89. MS (MALDI-TOF): calcd. for C₃₆H₄₀Br₂N₄S₄Si [M]⁺: 842.03; found, 843.991.

Compound DADAD. Compound dBr-ADA (0.271 g, 0.32 mmol), Compound 3 (0.465 g, 0.80 mmol) and Pd₂(dba)₃ (1.28 mol %) and P(*o*-Tol)₃ (5.12 mol%) were dissolved in 30 mL of dry toluene. The mixture was stirred overnight at 100 °C, the solvent was evaporated and the product was purified by column chromatography on silica with petroleum ether/dichloromethane (20/1 in v/v) as the eluent. The solvent was evaporated and compound DADAD was obtained as a deep blue viscous oil (0.2 g, 41 %). ¹H NMR (300 MHz, CDCl₃) δ= 8.11 (s, 2H), 7.83 (s, 2H), 7.37 (s, 4H), 7.34 (d, *J* = 4.8 Hz, 2H), 7.11 (d, *J* = 4.8 Hz, 2H), 1.50-0.80 (m, 102H); ¹³C NMR (75 MHz, CDCl₃) δ= 152.50, 150.77, 150.61, 149.25, 143.80, 142.99, 142.45, 141.25, 140.21, 130.12, 129.77, 125.97, 125.78, 125.52, 125.06, 124.92, 33.73, 33.24, 33.19, 31.87, 29.69, 29.21, 28.95, 24.23, 22.99, 22.64, 14.06, 12.02, 11.96. MS (MALDI-TOF): calcd. for C₈₄H₁₁₄N₄S₈Si₃ [M]⁺: 1518.61; Found, 1518.588.

3. Results and discussion

3.1. Synthesis and characterization

The detailed synthetic routes of all intermediates and target oligomers are shown in Scheme 1. The oligomer **DA** can be prepared straightforwardly from the starting materials of 4-bromo-2,1,3-benzothiadiazole (**1**) and 4,4'-bis(*n*-octyl)-5-trimethyltin-dithieno[3,2-*b*:2',3'-*d*]silole (**3**)²⁸ on the basis of a palladium-catalyzed Stille cross-coupling reaction. The target oligomer **ADA** was synthesized in a moderate yield by using compound **1** and 4,4'-bis(*n*-octyl)-5,5'-bis(trimethyltin)-dithieno[3,2-*b*:2',3'-*d*]silole (**4**)²⁸ as the starting materials. The analogues synthetic procedure by using compound **3**²⁸ and 4,7-dibromo-2,1,3-benzothiadiazole (**2**)²⁹ as the starting materials give the target oligomer **DAD**. The higher molecular weight oligomer **DADAD** was synthesized in a moderate yield based on the Stille cross-coupling reaction of compound **3** with the intermediate 7,7'-(4,4'-diethyl-4*H*-silolo[3,2-*b*:4,5-*b'*]dithiophene-2,6-diyl)bis(4-bromobenzo[*c*][1,2,5]thiadiazole) (**dBr-ADA**).



Scheme 1. Synthesis of oligomers

All resulted oligomers can be readily dissolved in common organic solvents including dichloromethane, tetrahydrofuran, chloroform, chlorobenzene, and so forth. The molecular structures of all target oligomers were confirmed by high-resolution matrix-assisted laser desorption ionization time of flight (MALDI-TOF) mass spectra (Fig. 1) and nuclear magnetic resonance (NMR) spectroscopy. Thermal gravimetric analysis (TGA) indicates that all oligomers have excellent thermal stability, with 5% weight loss temperature ($T_d^{5\%}$) higher than 340 °C (Table 1).

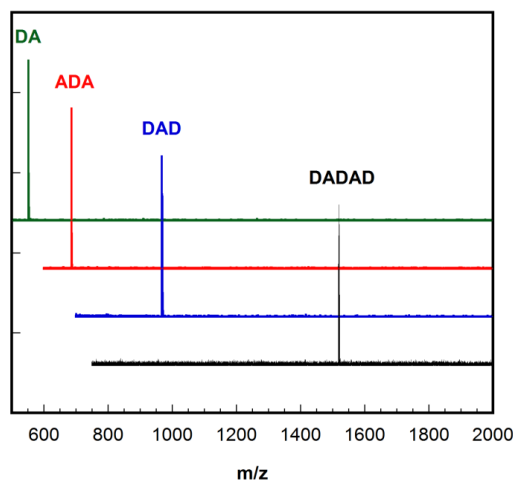


Fig. 1 MALDI-TOF spectra of oligomers

Table 1. Optical and thermal properties of the oligomers

Oligomers	T_d (°C)	λ_{max}^a (nm)	ϵ ($cm^{-1} M^{-1}$)	λ_{max}^b (nm)	$E_g^{opt c}$ (eV)
DA	341	451	13 000	N/A	N/A
ADA	384	491	18 800	516	2.40
DAD	396	537	23 900	547	2.27
DADAD	419	596	30 800	606	2.05

^a The maximum absorption in dichloromethane solution;

^b The maximum absorption as thin films;

^c The optical band-gap estimated from the absorption onset as thin films.

3.2. Optical properties

Fig. 2 illustrates the UV-vis absorption spectra of oligomers in dichloromethane solution with concentration of $2 \times 10^{-5} mol L^{-1}$ and as thin films. The absorption spectra of these oligomers exhibited dual-band characteristics as typical D–A-type of conjugated chromophores, where the less intense high-energy band with maximum absorbance (λ_{max}) of 350–380 nm corresponded to the characteristic $\pi-\pi^*$ transition and the featureless low-energy absorbance attributed to the intramolecular charge transfer (ICT) transition.^{12,22,30} It was also observed that the low-energy absorbance gradually shifted from 451 nm for **DA** to 596 nm for **DADAD** (Fig. 2a), implying the greatly extended π -conjugation with the increased molecular size. The comparison of the absorption profiles of **ADA** and **DAD** in Fig. 2a demonstrated a 46 nm bathochromic shift of the **DAD** chromophore, and the molar absorptivity also increased from 18 800 $cm^{-1} M^{-1}$ of **ADA** to 23 900 $cm^{-1} M^{-1}$ of **DAD**, illustrating the higher delocalization of π -conjugation in **DAD** chromophore. The highest molar absorptivity of 30 800 $cm^{-1} M^{-1}$ was realized for **DADAD** that have the longest π -conjugation.

The absorption profiles as thin films in Fig. 2b were normalized due to the variation of film thickness. One can observe the slight red-shift of ~10 nm along with the broadening of the absorbance at long-wavelength band. It was also recognized that the absorption profile of **ADA** exhibited much more pronounced bathochromic shift with the emergence of the fine structures at 559 nm, which can be attributed to the aggregation in solid state that was owing to the strong intermolecular interaction of the electron-

withdrawing BT units. The optical band gap as estimated from the absorption onset of thin films were in the range of 2.05–2.40 eV. Detailed optical properties data were summarized in Table 1.

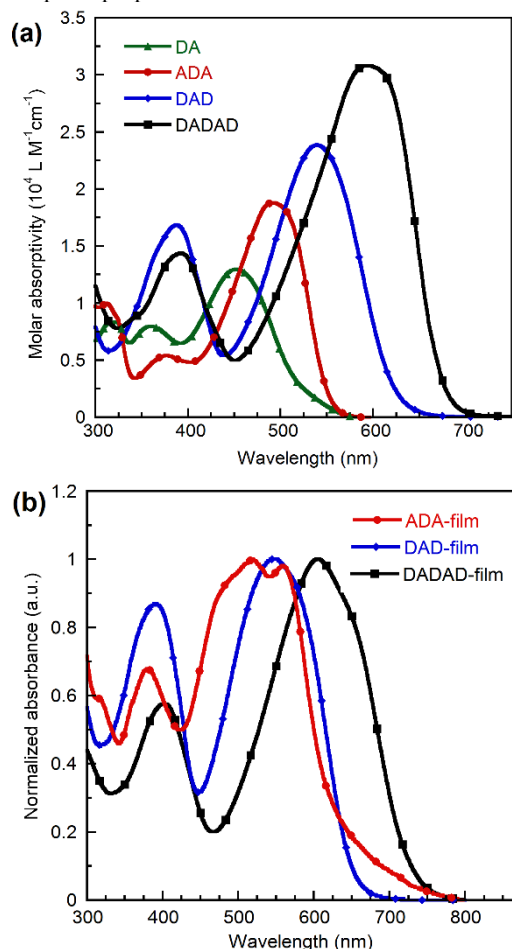


Fig. 2 UV-vis spectra of oligomers in dichloromethane solution (2×10^{-5} mol L⁻¹) (a) and as thin films (b)

3.3. Electrochemical properties and theoretical calculations

The electrochemical properties of oligomers were investigated to elucidate the frontier molecular orbital energy levels. The measurements were carried out in dichloromethane solution by using 0.1 M *n*-tetrabutylammonium hexafluorophosphate as the supporting electrolyte at a scan rate of 50 mV s⁻¹.³¹ The CV characteristics of these oligomers were illustrated in Fig. 3 and relevant data were summarized in Table 2. With respect to the reference of ferrocene/ferrocenium (Fc/Fc⁺), the onsets of oxidation potential (E_{ox}) and reduction potential (E_{red}) of oligomers were determined to be in the range of 0.17 ~ 0.51 V and -1.64 ~ -1.82 V, respectively. Assuming the redox potential of Fc/Fc⁺ to be -4.80 eV relative to the vacuum level, the highest occupied molecular orbitals (E_{HOMO}) and the lowest unoccupied molecular orbitals (E_{LUMO}) energy levels can be calculated by using the equation of $E_{\text{HOMO}} = -(E_{\text{ox}} + 4.80)$ eV and $E_{\text{LUMO}} = -(E_{\text{red}} + 4.80)$ eV, respectively.³² Accordingly, the calculated E_{HOMO} and E_{LUMO} of these oligomers were in the range of -5.31 ~ -4.97 eV and -3.16 ~ -2.98 eV, respectively. It is worth noting that with the elongation of conjugated length, both E_{HOMO} and E_{LUMO} gradually converged to conjugated DTS-BT based polymer^{22,33}. Similar situation also

exists in other π -conjugated small molecule systems.¹⁸ The calculated electrochemical band gap was in the range of 1.80–2.33 eV.

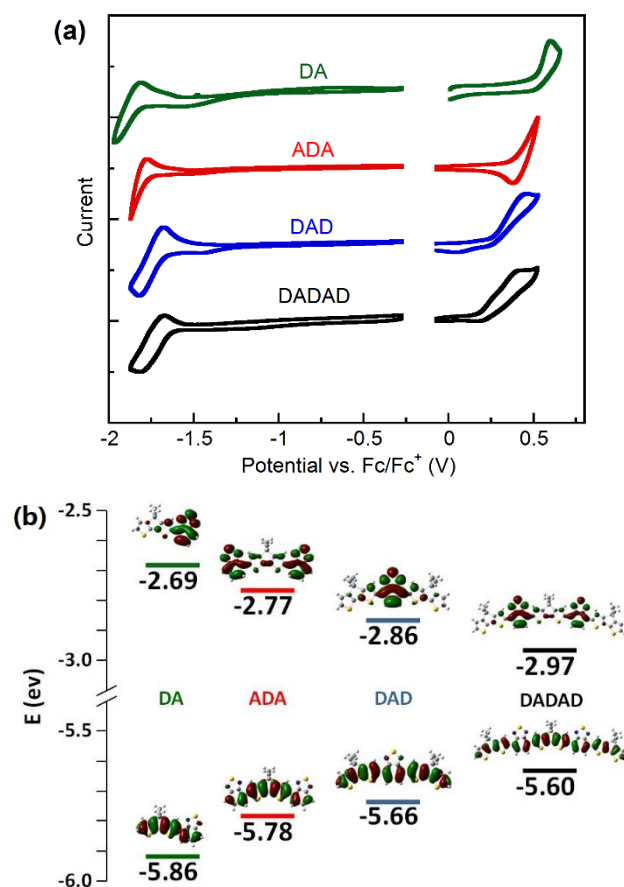


Fig. 3 Cyclic voltammograms of oligomers measured in CH₂Cl₂ solution (a); contour plots of molecular frontier orbitals and HOMO/LUMO energy levels based on DFT calculations (b)

Table 2. Electrochemical properties and calculated frontier molecular orbitals of oligomers

Oligomer	DA	ADA	DAD	DADAD
$E_{\text{ox}}^{\text{CV}}$ (V)	0.80	0.75	0.68	0.50
$E_{\text{red}}^{\text{CV}}$ (V)	-1.61	-1.69	-1.77	-1.81
$E_{\text{HOMO}}^{\text{CV}}$ (eV)	-5.60	-5.55	-5.48	-5.30
$E_{\text{LUMO}}^{\text{CV}}$ (eV)	-3.19	-3.11	-3.03	-2.99
E_{g}^{CV} (eV)	2.41	2.44	2.45	2.31
HOMO^{DFT} (eV)	-5.86	-5.78	-5.66	-5.60
LUMO^{DFT} (eV)	-2.69	-2.77	-2.86	-2.97
$E_{\text{g}}^{\text{DFT}}$ (eV)	3.17	3.01	2.80	2.63

To further understand the molecular orbital geometry and electrical properties of these small molecules, density functional theory (DFT) theoretical calculations were carried on the basis of the restricted B3LYP/6-311G (d) function by using Gaussian 09 package.³⁴ In order to simply the calculation, the alkyl side chains were replaced by methyl groups for all oligomers. Fig. 3b

illustrated the calculated HOMO and LUMO levels of the resulted oligomers. It was realized that for all oligomers, the HOMO is delocalized along the π -conjugated architectures, while the LUMO is mainly located at the electron-deficient BT units. As anticipated, the calculated HOMO levels gradually increased while the LUMO levels progressively decreased with the elongation of π -conjugation. The combination of these factors leads to gradually narrowed band gaps with the extension of π -conjugation, which is in good agreement with the measured optical and electrochemical results. The detailed calculated parameters are summarized in Table 2.

3.4 Photovoltaic properties

Photovoltaic properties of the resulting oligomers were investigated by fabricating solar cells with inverted device structure of ITO/PFN-OX/oligomer:PCBM/MoO₃/Al. The photoactive layer comprised oligomer:PCBM with optimized weight ratio of 1:2. Here a thin layer of poly[9,9-bis(6,6'-(*N,N*-diethylamino)hexyl)fluorene-*alt*-9,9-bis(3-ethyl(o)oxetane-3-ethyloxy)hexyl)-fluorene] (PFN-OX) was spin-casted on the top of ITO and facilitate electron-collection.²⁶ The photovoltaic performances of copolymers were measured under a simulated AM 1.5G illumination of 100 mW cm⁻². The current density–voltage (J - V) characteristics and external quantum efficiency (EQE) spectra were shown in Fig. 4, and corresponding photovoltaic parameters were summarized in Table 3.

Initial organic solar cells measurements by using PC₆₁BM as the electron acceptor exhibited comparatively low performances, which exhibited the power conversion efficiency (PCE) in the range of 0.31–0.63%. The replacement of PC₆₁BM by PC₇₁BM leads to slightly improved device performance in terms of increased short circuit current (J_{SC}). The fact can be attributed to the much stronger absorption of PC₇₁BM in the visible region than PC₆₁BM, which can compensate the absorption valley of the polymers and beneficial for improved efficiency³⁵. The best device performance was achieved based on **DADAD:PC₇₁BM** as the photoactive layer, which showed a moderate PCE = 1.12% (V_{OC} = 0.81 V, J_{SC} = 4.70 mA cm⁻², and FF = 30.1%). To confirm the photo-response and the accuracy of J_{SC} measurements, the external quantum efficiencies (EQE) characteristics were recorded as shown in Fig. 4b. It was noted that all devices exhibited the moderate EQE in the range of 400–750 nm, where the device based on **DADAD** showed the much higher EQE than the others. The integrals of the EQEs of all oligomers were in good accordance with the J_{SC} values.

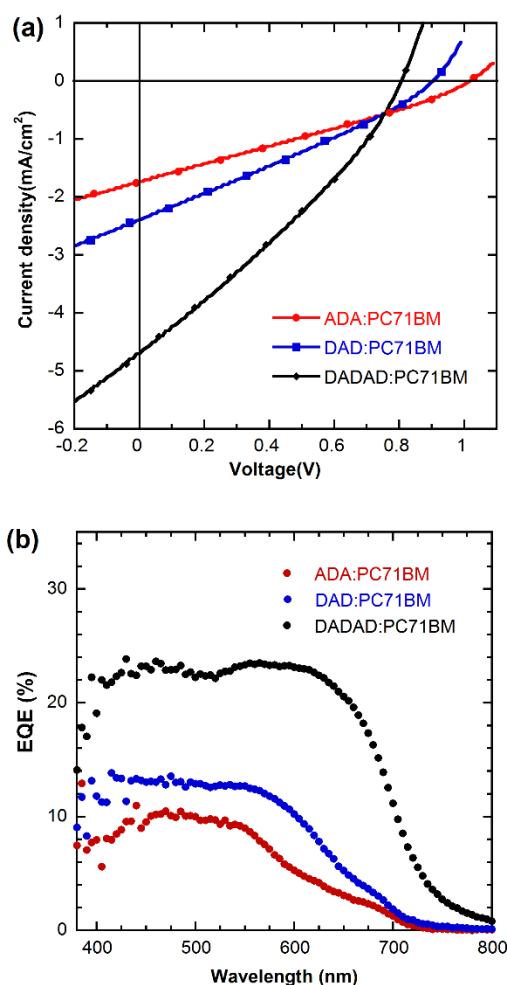


Fig. 4 J - V characteristics (a) and EQE spectra (b) of solar devices with device architecture of ITO/PFN-OX/oligomer:PC₇₁BM/MoO₃/Al under the illumination of AM 1.5G from a solar simulator (100 mW cm⁻²)

Table 3. Photovoltaic performances of oligomers

Oligomer	J_{SC} (mA/cm ²)	V_{OC} (V)	FF (%)	PCE (%)
ADA:PC ₆₁ BM	1.14	0.94	28.6	0.31
DAD:PC ₆₁ BM	1.64	0.93	28.4	0.43
DADAD:PC ₆₁ BM	2.76	0.81	28.7	0.64
ADA:PC ₇₁ BM	1.74	1.02	28.2	0.50
DAD:PC ₇₁ BM	2.40	0.90	28.6	0.62
DADAD:PC ₇₁ BM	4.70	0.81	30.1	1.12

3.5 Film morphology

To get insight into the influence of film morphology on device performance, the surface topography of oligomers:PC₇₁BM films were measured by atomic force microscopy. The bulk heterojunction films were fabricated by spin-casting the oligomer:PC₇₁BM on the top of the ITO/PFN-OX substrate, which followed exactly the same conditions as those for device

measurements. Fig. 5 illustrated the surface topography of oligomers:PC₇₁BM films. From Fig. 5a one can clearly observe the rough morphology of DA:PC₇₁BM with root-mean-square (RMS) roughness value of 1.53 nm, where the serious phase separation can be attributed to the relatively poor miscibility of the DA and PC₇₁BM. As the film morphology played a critical role in charge transport cross the bulk heterojunction films, the serious phase separation along with the coarse-grained feature of DA:PC₇₁BM is detrimental to the photovoltaic performances. In contrast, much smoother topography was realized for the BHJ films of ADA:PC₇₁BM (Fig. 5b) and DAD:PC₇₁BM (Fig. 5c), which exhibited comparable RMS of 0.41 and 0.61 nm, respectively. The improved surface morphology implied better miscibility with PC₇₁BM, which was positive for the charge carrier transportation in the relevant photovoltaic devices. The blend film of DADAD:PC₇₁BM also exhibited relatively smooth surface along with the emergence of percolating fibrous features across the whole film, which was essentially favorable for charge transportation and can effectively reduce charge recombination and traps. We note that the performances of these resulting devices are relatively low, nonetheless, these observations of AFM images illustrated that the film morphology can be optimized by the molecular architecture, which can provide an effective hint for the future molecules design.

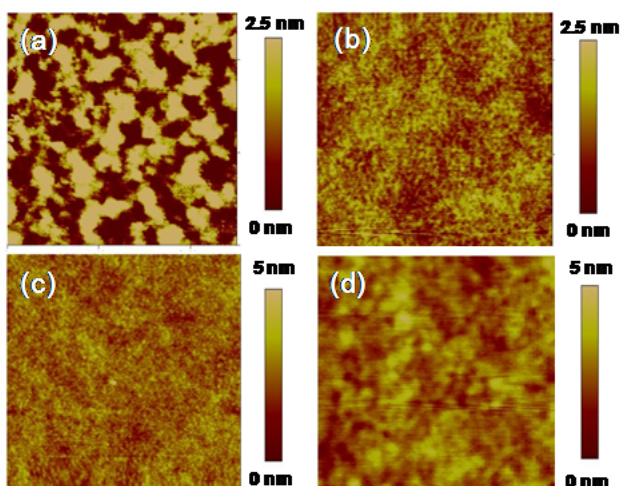


Fig. 5 AFM images ($2.5 \mu\text{m} \times 2.5 \mu\text{m}$) of oligomers:PC₇₁BM blend films with weight ratio of 1:2; DA (a), ADA (b), DAD (c) and DADAD (d)

4. Conclusions

In summary, a series of donor-acceptor type of conjugated oligomers comprising dithienosilole as the donor unit and benzothiadiazole as the acceptor unit were synthesized via Stille coupling reaction. Despite these oligomers contain the same donor and acceptor moieties along the conjugated architectures, they are structurally different in terms of the ratio of donor or acceptor segments, resulting in the significantly different absorption spectra, frontier molecular orbitals, and phase separation of the bulk-heterojunction films. Organic solar cells fabricated on the basis of these chromophores exhibited moderate power conversion efficiencies, in which the device based on higher molecular weight oligomer exhibited superior performances to lower molecular

weight counterparts. The results demonstrated that the extending π -conjugation of chromophores can be an effective molecular design strategy for achieving improved photovoltaic performance.

Acknowledgments

This work was financially supported by the Ministry of Science and Technology (No. 2014CB643501), the Natural Science Foundation of China (Nos. 51303056, 21125419, 50990065, and 51010003), and the Guangdong Natural Science Foundation (No. S2012030006232).

Notes and references

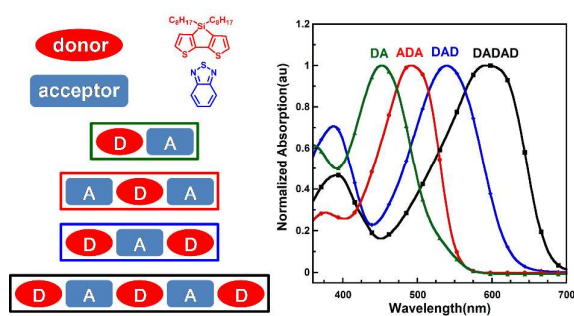
^a State Key Laboratory of Luminescent Materials and Devices, and Institute of Polymer Optoelectronic Materials and Devices, South China University of Technology, Guangzhou 510640, China. Fax: 86 20 87110606; Tel: 86 20 87114346; E-mail: msfhuang@scut.edu.cn (F. Huang), msleiyang@scut.edu.cn (L. Ying)

† Electronic Supplementary Information (ESI) available: The ¹H-NMR, ¹³C-NMR of all intermediates and target oligomers. See DOI: 10.1039/b000000x

- G. Yu, J. Gao, J. C. Hummelen, F. Wudl and A. J. Heeger, *Science*, 1995, **270**, 1789-1791.
- S. Gunes, H. Neugebauer and N. S. Sariciftci, *Chem. Rev.*, 2007, **107**, 1324-1338.
- B. C. Thompson and J. M. J. Fréchet, *Angew. Chem. Int. Edit.*, 2008, **47**, 58-77.
- Z. C. He, C. M. Zhong, S. J. Su, M. Xu, H. B. Wu and Y. Cao, *Nat. Photonics*, 2012, **6**, 591-595.
- M. Wang, X. W. Hu, P. Liu, W. Li, X. Gong, F. Huang and Y. Cao, *J. Am. Chem. Soc.*, 2011, **133**, 9638-9641.
- W. Li, A. Furlan, K. H. Hendriks, M. M. Wienk and R. A. J. Janssen, *J. Am. Chem. Soc.*, 2013, **135**, 5529-5532.
- J. You, L. Dou, K. Yoshimura, T. Kato, K. Ohya, T. Moriarty, K. Emery, C.-C. Chen, J. Gao, G. Li and Y. Yang, *Nat Commun.*, 2013, **4**, 1446.
- Y. Liu, J. Zhao, Z. Li, C. Mu, W. Ma, H. Hu, K. Jiang, H. Lin, H. Ade and H. Yan, *Nat Commun.*, 2014, **5**, 5293.
- J. Roncali, *Chem. Rev.*, 1997, **97**, 173-206.
- D. Liu, M. Xiao, Z. Du, Y. Yan, L. Han, V. A. L. Roy, M. Sun, W. Zhu, C. S. Lee and R. Yang, *J. Mater. Chem. C*, 2014, **2**, 7523-7530.
- J. N. Cao, X. Y. Du, S. Chen, Z. Xiao and L. M. Ding, *Phys. Chem. Chem. Phys.*, 2014, **16**, 3512.
- Y. Sun, G. C. Welch, W. L. Leong, C. J. Takacs, G. C. Bazan and A. J. Heeger, *Nat. Mater.*, 2012, **11**, 44-48.
- H.-Y. Chen, J. Hou, A. E. Hayden, H. Yang, K. N. Houk and Y. Yang, *Adv. Mater.*, 2010, **22**, 371-375.
- T.-Y. Chu, J. Lu, S. Beaupré, Y. Zhang, J.-R. Pouliot, J. Zhou, A. Najari, M. Leclerc and Y. Tao, *Adv. Funct. Mater.*, 2012, **22**, 2345-2351.
- J. Zhou, Y. Zuo, X. Wan, G. Long, Q. Zhang, W. Ni, Y. Liu, Z. Li, G. He, C. Li, B. Kan, M. Li and Y. Chen, *J. Am. Chem. Soc.*, 2013, **135**, 8484-8487.
- J. Zhou, X. Wan, Y. Liu, Y. Zuo, Z. Li, G. He, G. Long, W. Ni, C. Li, X. Su and Y. Chen, *J. Am. Chem. Soc.*, 2012, **134**, 16345-16351.
- J. Zhou, X. Wan, Y. Liu, G. Long, F. Wang, Z. Li, Y. Zuo, C. Li and Y. Chen, *Chem. Mater.*, 2011, **23**, 4666-4668.
- C. Zhou, Y. Liang, F. Liu, C. Sun, X. Huang, Z. Xie, F. Huang, J. Roncali, T. P. Russell and Y. Cao, *Adv. Funct. Mater.*, 2014, **24**, 7538-7547.
- Y. Chen, X. Wan and G. Long, *Acc. Chem. Res.*, 2013, **46**, 2645-2655.
- C. Kim, J. Liu, J. Lin, A. B. Tamayo, B. Walker, G. Wu and T.-Q. Nguyen, *Chem. Mater.*, 2012, **24**, 1699-1709.
- X. Liu, Y. Sun, L. A. Perez, W. Wen, M. F. Toney, A. J. Heeger and G. C. Bazan, *J. Am. Chem. Soc.*, 2012, **134**, 20609-20612.

22. L. Zhang, N. S. Colella, F. Liu, S. Trahan, J. K. Baral, H. H. Winter, S. C. B. Mannsfeld and A. L. Briseno, *J. Am. Chem. Soc.*, 2012, **135**, 844-854.
23. J. H. Hou, H. Y. Chen, S. Q. Zhang, G. Li and Y. Yang, *J. Am. Chem. Soc.*, 2008, **130**, 16144-16145.
24. X. F. Liu, Y. M. Sun, B. B. Y. Hsu, A. Lorbach, L. Qi, A. J. Heeger, and G. C. Bazan, *J. Am. Chem. Soc.*, 2014, **136**, 5697-5708.
25. X. Liu, B. B. Y. Hsu, Y. Sun, C.-K. Mai, A. J. Heeger and G. C. Bazan, *J. Am. Chem. Soc.*, 2014, **136**, 16144-16147.
26. Y. Dong, X. Hu, C. Duan, P. Liu, S. Liu, L. Lan, D. Chen, L. Ying, S. Su, X. Gong, F. Huang and Y. Cao, *Adv. Mater.*, 2013, **25**, 3683-3688.
27. S. Liu, K. Zhang, J. Lu, J. Zhang, H.-L. Yip, F. Huang and Y. Cao, *J. Am. Chem. Soc.*, 2013, **135**, 15326-15329.
28. P. M. Beaujuge, H. N. Tsao, M. R. Hansen, C. M. Amb, C. Risko, J. Subbiah, K. R. Choudhury, A. Mavrinskiy, W. Pisula, J.-L. Brédas, F. So, K. Müllen and J. R. Reynolds, *J. Am. Chem. Soc.*, 2012, **134**, 8944-8957.
29. K. Pilgram, M. Zupan and R. Skiles, *J. Heterocycl. Chem.*, 1970, **7**, 629-633.
30. Y. Hou, Y. Chen, Q. Liu, M. Yang, X. Wan, S. Yin and A. Yu, *Macromolecules*, 2008, **41**, 3114-3119.
31. D. Demeter, T. Rousseau, P. Leriche, T. Cauchy, R. Po and J. Roncali, *Adv. Funct. Mater.*, 2011, **21**, 4379-4387.
32. M. Wang, X. W. Hu, L. Q. Liu, C. H. Duan, P. Liu, L. Ying, F. Huang and Y. Cao, *Macromolecules*, 2013, **46**, 3950-3958.
33. R. C. Coffin, J. Peet, J. Rogers and G. C. Bazan, *Nat Chem*, 2009, **1**, 657-661.
34. M. J. Frisch, G. W. Trucks, H. B. Schlegel, G. E. Scuseria, M. A. Robb, J. R. Cheeseman, G. Scalmani, V. Barone, B. Mennucci, G. A. Petersson, H. Nakatsuji, M. Caricato, X. Li, H. P. Hratchian, A. F. Izmaylov, J. Bloino, G. Zheng, J. L. Sonnenberg, M. Hada, M. Ehara, K. Toyota, R. Fukuda, J. Hasegawa, M. Ishida, T. Nakajima, Y. Honda, O. Kitao, H. Nakai, T. Vreven, J. A. Montgomery, Jr, J. E. Peralta, F. Ogliaro, M. Bearpark, J. J. Heyd, E. Brothers, K. N. Kudin, V. N. Staroverov, R. Kobayashi, J. Normand, K. Raghavachari, A. Rendell, J. C. Burant, S. S. Iyengar, J. Tomasi, M. Cossi, N. Rega, J. M. Millam, M. Klene, J. E. Knox, J. B. Cross, V. Bakken, C. Adamo, J. Jaramillo, R. Gomperts, R. E. Stratmann, O. Yazyev, A. J. Austin, R. Cammi, C. Pomelli, J. W. Ochterski, R. L. Martin, K. Morokuma, V. G. Zakrzewski, G. A. Voth, P. Salvador, J. J. Dannenberg, S. Dapprich, A. D. Daniels, O. Farkas, J. B. Foresman, J. V. Ortiz, J. Cioslowski and D. J. Fox, Gaussian 09, Revision D.01, Gaussian, Inc., Wallingford CT, 2009.
35. M. M. Wienk, J. M. Kroon, W. J. H. Verhees, J. Knol, J. C. Hummelen, P. A. van Hal and R. A. J. Janssen, *Angew. Chem. Int. Edit.*, 2003, **42**, 3371-3375.

Graphical Abstract



The investigations provide a distinctive view to observe how relevant optoelectronic properties change of oligomers with different molecular sizes.